Defence Science Journal, Vol. 74, No. 4, July 2024, pp. 482-489, DOI : 10.14429/dsj.74.18716

Performance Evaluation of DGNSS Receiver for Dynamic Military Applications

Moiz Chasmai*, Gagandeep Purohit, Arun Barde, Sandeep, Prashant Kumar and Abhijit Kamble

DRDO-Research & Development Establishment (Engineers), Pune – 411015, India
**E-mail: moizc.rde@gov.in*

ABSTRACT

In military applications, a highly accurate and precise navigation system is necessary for some ground-based combat system applications to navigate the vehicle and mark the location of the fuses and pickets laid by the mobile equipment. Few companies across the globe have developed expertise in manufacturing Global Navigation Satellite System (GNSS) receivers with Real Time Kinematics (RTK) capability along with integrated INS. On mobile equipment, it is not always possible to precisely place the Differential GNSS (DGNSS) antenna and GNSS receiver at the point for which the data needs to be marked. For such applications, lever arm calculation needs to be implemented. Also, due to uneven terrain conditions and slopes, the vehicle undulates up to 10° about its longitudinal and transverse axis. This dynamic condition induces considerable errors in the actual data. During the fuse laying process, there is also a continuous requirement for real-time location data in the GNSS-denied environment for a short period. INS was integrated with the GNSS receiver. We discuss test methodology for GNSS receiver performance evaluation. Experimentations were performed, taking into consideration these requirements. Data collected are also analyzed and discussed. Test results confirmed that the module is accurate with an accuracy of a few centimeters.

Keywords: DGNSS; Lever arm; Location marking; Rover; INS

NOMENCLATURE

v_{GNSS} : Measurement noises of GPS
r_b : Offset from INS to GNSS antenna resolved in the body frame
R_m : Meridian of curvature of the earth ellipsoid
R_t : Normal radii of curvature of the earth ellipsoid
$[L\ l\ h]^T$: Position vector P in the local tangent plane

1. INTRODUCTION

GNSS is a well-known technology for navigation and 3D positioning over the globe. It is used in vast applications, including navigation of ground equipment, vessels and space applications[1]. Existing constellations are Global Positioning System (GPS) developed by the USA, Global'naya Navigatsiomaya Sputnikova Sistema (GLONASS) developed by Russia[2], Europe's Galileo and China's BeiDou 2. Japan's Quasi-Zenith Satellite System (QZSS), China's BeiDou 1 and Indian Regional Navigational Satellite System (IRNSS) are regional systems[3].

Low-cost GNSS solutions are used in applications like monitoring bridges and dams for their structural health and the guidance of agricultural machines[4], robotic equipment, UAVs, and other vehicles[5]. However, the shortcoming of the low-cost GNSS receivers is that these receivers are mostly single frequency, leading to a longer time for ambiguity resolution, which leads to a longer time to reduce the errors[6-7]. The velocity of a moving platform can also be estimated quite accurately using different constellations in open and urban environments[8].

Received : 06 December 2022, Revised : 13 September 2023
Accepted : 30 January 2024, Online published : 24 July 2024

In military ground-based applications, there are requirements to plan the route, navigate the systems along a pre-planned route, lay evenly spaced fuses under the surface, generate a map along with marking and retrieve the fuses when required with an accuracy of a few decimeters. Differential GNSS is used, where high accuracy is critical for the system's overall functionality. It eliminates atmospheric and clock errors. In GNSS, the receiver matches its internal pseudocode with the one it receives. DGNSS gives an accuracy in the range of 50-100 cm. However, in a dynamic platform, this accuracy may further degrade. The carrier phase enhancement technique is used instead of pseudocode for further accuracy enhancement. The carrier phase changes at a rate of more than 1000 times compared to the phase change of pseudocode. However, the difficulty with this technique is aligning the signals. Misalignment of carrier phase between the receiver-generated signal & satellite signal is an integer multiple of carrier wavelength. This problem is called the Integer Ambiguity problem. RTK[9] requires the resolution of integer ambiguity. The receiver uses LAMBDA, QR-transform, LU decomposition or other methods to calculate the integer number of wavelengths between satellites and the receiver. However, if the lock with the particular satellite is lost, after resolving integer ambiguity, the mode changes from RTK fix to RTK float.

When the system gets integrated with the mobile platform, multiple issues add to the actual error of the receiver.

One of the issues is that, it is sometimes practically not feasible to precisely mount the GNSS receiver antenna at the location whose position is required. In such cases, lever arm

correction is applied to estimate the actual location of the fuse concerning the receiver antenna position. A GNSS lever arm correction aims to relate the antenna position with respect to fuse position. While implementing the lever-arm corrections, uncertainty in the location calculation of the object is an important error source during the integration of the GNSS on the mobile platform.

Another issue is due to uneven terrain conditions and slopes. The vehicle undulates up to 10o about its longitudinal and transverse axes, which causes a large amount of error in the actual fuse location measurement. It requires slope error correction using INS in real time to eliminate the offset.

Since ground vehicles travel in surroundings with poor satellite visibility, a low-cost single constellation receiver may lead to frequent satellite-receiver link breakage. Multi-band receivers can support multiple constellations and take SBAS corrections like GAGAN in such applications.

Also, there is a requirement to mark the location of the fuses, even in the case of a GNSS-denied environment, without halting the mission. In such a case, INS is required with the GNSS receiver to ascertain the location with some error for a small duration before the GNSS network gets restored.

This exercise aims to evaluate the performance of the GNSS receiver with RTK and integrated INS and deliver decimeter-level relative positioning, considering lever arm and slope error corrections. Performance of the equipment has been evaluated in a GNSS-denied environment. INS includes 3-axis accelerometer, 3-axis magnetometer and 3-axis gyroscopes. Acceleration range is ±16 g with acceleration bias instability of <15 µg, angular rate range is ±450 °/s with angular bias instability of 0.8 °/hr, roll range is ±180° with accuracy of 0.06° RMS, pitch range is ±90° with accuracy of 0.1° RMS and heading range is ±180° with accuracy of <0.3° RMS with GPS in dynamic conditions and <0.5° RMS with magnetometer. Angle resolution is <0.01° & magnetometer range is ±8 gauss.

2. SYSTEM CONFIGURATION

The GNSS-based fuse location recording system consists of a base station and a rover as shown in Fig. 1. The base station consists of a GNSS receiver with antenna and VHF Radio Modem with antenna. The Rover carries a GNSS receiver with an antenna, a VHF Radio Modem with an antenna and a Geographical Mapping System (GMS) Laptop.

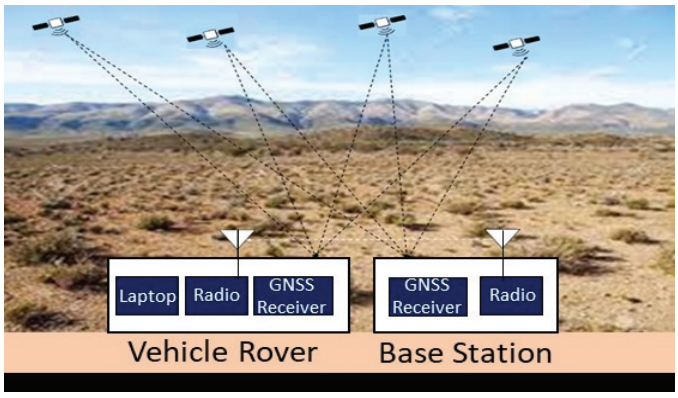

Figure 1. System configuration.

The GNSS receiver module used for evaluation consists of a power block, GNSS processor, IO Processor, RF block and communication block. The GNSS processor block consists of a multi-band Septentrio Mosaic GNSS chipset that supports multi-frequency L1/L2/L5 satellite signal reception and is powerful enough to track up to 400 satellites. It also applies RTK corrections to compute an accurate position. The IO Processor decodes GNSS messages and sends processed data on various interfaces. It also receives configuration commands and sets the required configuration in the device like serial/COM port baud rates, update rate, GNSS configuration (constellations), RTK configuration – message formats and any other settings. The communication module supports multiple serial RS232 ports for communication with the GNSS. One RS232 port receives differential corrections from the base station over an external RF link. The device also has an Ethernet port for data output and configuration. The GNSS receiver is given power by a 12/24V battery for which the receiver has a DC-DC converter for power isolation and an EMI filter for necessary EMI protection. The receiver is housed in a lightweight IP65 enclosure to be carried by field personnel.

Calamp Viper SC+ VHF Radio modems transmit the base error correction data to the receiver over a serial link for further processing. Base station Radio modem collects error correction data from the receiver over a serial link and sends it through the air on a VHF link. The vehicle rover radio modem receives this error correction data and provides it to the receiver over a serial link for further processing.

GMS is a user interface application loaded on a rugged laptop to plan, navigate and mark the location of the laid fuses. A base station and Vehicle Rover communicate with the satellites and evaluate their respective location data. In differential mode, the base station transmits the error correction data to the rover in real time to correct its relative position. It is a carrier phase measurements based technique and the transmission of corrections from the base station, whose location is well known, to the rover mounted on vehicle. Here, the absolute errors that affect the static positioning cancels out.

3. PERFORMANCE EVALUATION

In defence ground-based applications, there is a necessity for a highly accurate and precise navigation and location marking system installed on a heavy-wheeled/ tracked vehicle as a subsidiary system of a hydroelectric-mechanical system. They have their dynamics that hamper the accuracy of the Vehicle GNSS receiver. The requirement arises to customize the GNSS receiver by reducing the errors generated through ground undulation, poor satellite visibility, GNSS-denied environment and GNSS antenna mounting position issues. A full-scale product functionality test was performed for the product considering GNSS with integrated INS module as a Rover Station and only GNSS module as a Base Station. These are the tests performed to validate the desired performance:

3.1 Static Condition Test in Standalone and RTK Modes to Validate the Accuracy

Initially, using a GNSS receiver, position errors were obtained with respect to two surveyed ground control points.

At one ground control point, the base station was established. The antenna (rover) was placed on another point. The baseline distance between the rover and the base station was 540m. The average error achieved by the experimentations conducted on this setup in RTK mode was 0.8 cm. After establishing the absolute error of the DGNSS receiver w.r.t. surveyed points, the same DGNSS receiver was used for locating non-surveyed points.

Points A, B, C, D and E were marked on the ground at a spacing of 3m each for carrying out the performance evaluation of the GNSS receiver in standalone mode without differential corrections. GNSS/INS Rover setup was established on the ground. The GNSS antenna was placed on the ground as shown in Fig. 2.

Figure 2. Placement of GNSS antenna on ground.

GNSS-INS integrated module has two outputs; pure GNSS & the GNSS-INS integrated output. The GNSS-fix data from GNSS output & GNSS-INS integrated output were collected. The distance between two points was calculated using the Haversine formula. This formula calculates the shortest distance between two points in the earth-centric spherical coordinate system[10]. The Haversine formula is used for navigating on the surface of a large circle irrespective of the earth's surface undulations. This formula11 uses the perturbation in Lat (Δlat) and Lon (Δlong) between two coordinate points in radians as given below.

$$\Delta Lat = Lat2 - Lat1 \quad (1)$$

$$\Delta Long = Long2 - Long1 \quad (2)$$

Using the two definitions above, we calculate the distance between two points using the formula in (3)[11].

$$Distance = 2 \times R \times arcsin \quad (3)$$

Where, R in (3) is the equatorial radius of the earth, that is 6378.137 km[12]. As, Δ latitudes and Δ longitudes are small for short distances, Eqn. (3) can be rewritten by removing sine. The errors in the distances were obtained, whose results are shown in Fig. 3. Here, e is the relative position error, calculated using the Haversine formula between the output of the given points when they are measured using GNSS only (without INS and RTK corrections) and GNSS-INS integrated (without RTK corrections). This error e represents the effect of INS when it is integrated into GNSS output. eAB/eBC/eCD/eDE represent the errors between two points on the ground using the Haversine formula. Here, RTK-correction was not used with GNSS-INS. Here, eAB represents the error in the distance between points

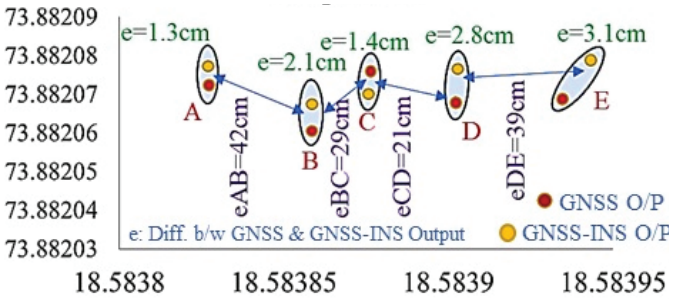

Figure 3. GNSS fix accuracy & INS data comparison.

A and B using GNSS-INS integrated output w.r.t. the actual value of 3 m.

To carry out the test to evaluate the accuracy of DGNSS in RTK mode with differential corrections, GNSS/INS Rover and Base Station were established on non-surveyed points on the ground by carrying out PPP[13-14] at the base station. Points A, B, C, D and E are on the ground at a spacing of 3m each. Four readings were collected at each point for RTK Fix and the distance errors were calculated using an average of all four values at a given point. Errors were calculated by comparing the on-ground distance between two points (3m) with the distance calculated between two points (based on the measured latitudes and longitudes of two adjacent points). Fig. 4 shows the results.

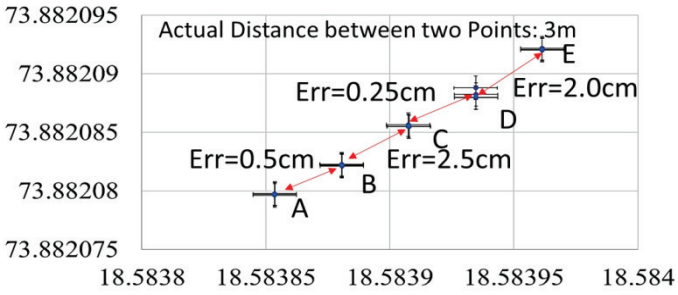

Figure 4. Accuracy in RTK mode.

Accuracy of GNSS in different modes was also evaluated by taking 25 sample readings at each point for each mode of operation. The box in the graph depicts the band of errors in the specific mode. The accuracy of position in different modes is given in Fig 5. The data measured in GNSS fix mode was beyond 1 Sigma. However, data measured in DGNSS, RTK float and RTK fix modes were in 1 Sigma, 2 Sigma and 3 Sigma respectively.

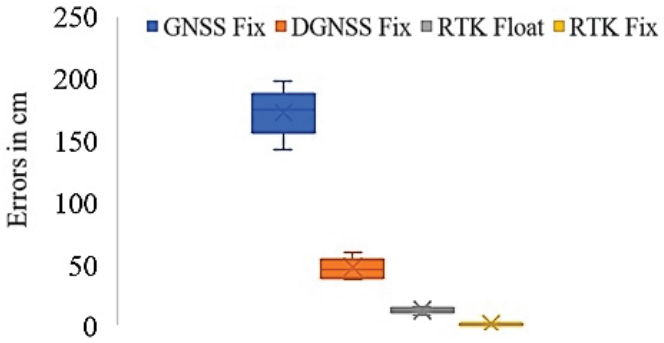

Figure 5. GNSS accuracy in different modes.

3.2 Ascertain the Update Rate and Starting Delays

- **Update Rate:** 50 Hz
- **Cold Start:** 25 sec for GNSS fix & 58 sec for RTK fix
- **Warm Start:** 2.5 sec for GNSS fix & 7 sec for RTK fix

These rates and timings are required for better performance in the dynamic applications.

3.3 Position Repeatability Test over Time Period

RTK Fix was acquired at a given position with the base station & rover in place. Twelve position measurement data were collected at regular intervals of 4 hr at a given point on the ground. The purpose of the tests was to validate acceptable repeatability in the position of 3.6 cm (1σ) while the constellation arrangements of GNSS satellites are changing with time, i.e., the geographical position of satellites is varying & new satellites may be acquired and measurements from previous satellites terminate. Fig. 6 shows the distribution of the location data of the position of the GNSS antenna during 48 hrs at regular intervals of 4 hrs.

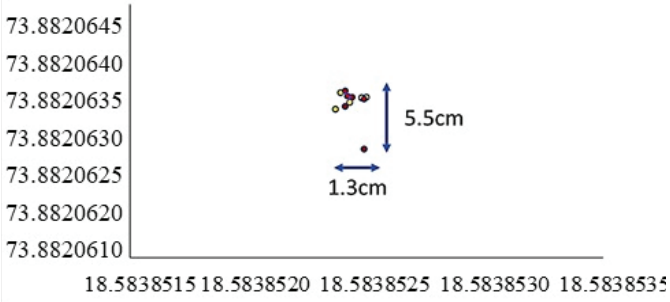

Figure 6. Position repeatability test over time period.

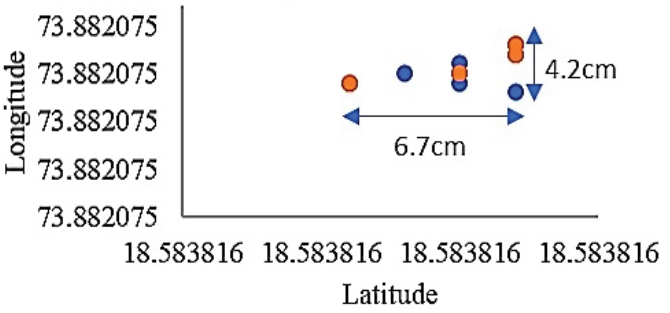

Figure 7. Position repeatability test after repositioning.

3.4 Position Repeatability Test After Repositioning

A dynamic test of the rover was done with respect to the ground frame. RTK fix was acquired at a given position 'A' (position measurements recorded). The rover roamed in the area within a radius of 100 mtr for 10 min. Then , it was later returned to the original position 'A'. Again, the position measurements were taken. Fig. 7 shows data collected for this test.

3.5 Position Repeatability Test After Fix Re-acquisition

Re-acquisition by turn-on/ turn-off is done to obtain positional measurements at a given position. Measurement is done once RTK was achieved by turning the system ON again after 30 min. Fig. 8 shows the distribution of the location data of the position of the GNSS antenna.

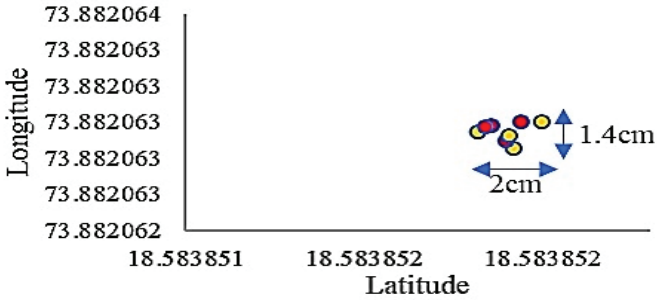

Figure 8. Position repeatability test after re-acquisition.

3.6 Evaluation of Time Taken During Re-powering and Re-acquisition in Different GNSS modes

GNSS/INS receiver was installed as per operational instructions. Initially, the power was disconnected from the GNSS/INS receiver, keeping the radio ON. After 10 minutes, the GNSS/INS receiver was turned ON. The timings were noted for different modes, i.e., GNSS, DGNSS, RTK Float and RTK. This test was repeated four times. The means of the results in each mode were calculated as depicted by the boxes. The results are shown in Fig. 9. The results show that the time taken for the GNSS fix mode is comparatively less. The algorithm complexity increases from GNSS fix mode to RTK fox mode. Hence, the time taken by the receiver to fix the mode also increases.

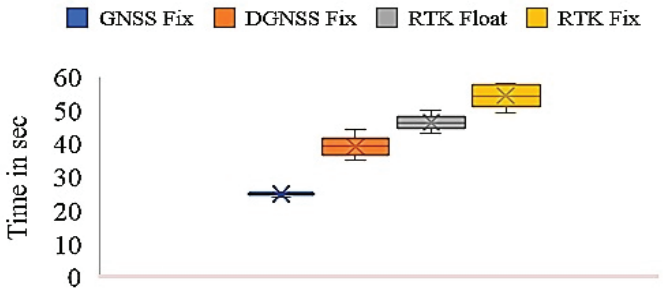

Figure 9. Time for mode fixing after e-powering.

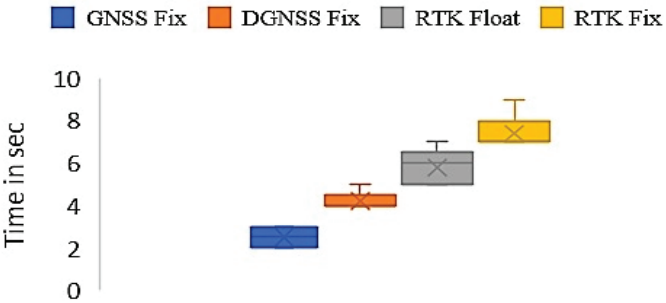

Figure 10. Time for mode fixing after re-acquisition.

Another test for the "time-to-fix" was carried out. GNSS antenna was disconnected and reconnected to measure the "time-to-fix". Times for different modes were noted, i.e., GNSS, DGNSS, RTK Float and RTK Fix as shown in Fig 10. It was repeated four times. The means of different modes depicted by the boxes in Fig. 10 were arrived at.

3.7 Test for Accuracy in Dynamic Condition

The Rover station, which includes the GNSS/INS receiver

and GNSS antenna, along with the radio modem, was mounted on a single plate, as shown in Fig. 11, so that the relative displacement between the GNSS/INS receiver and GNSS antenna is zero. This plate was then mounted on the roof of the object-laying vehicle.

Figure 11. GNSS receiver, radio and battery mounted on a single plate.

The rover was interfaced with the control unit over an Ethernet link on the vehicle. Four objects were laid on the ground at a distance of 3 m each along a straight line using this vehicle in moving condition. Whenever the object gets laid, the control unit records the location of the object using the current location data from the rover station. After all the four objects were placed on the ground, the location of these objects was measured using a DGNSS-based handheld rover in static conditions. The difference between the position estimated in the dynamic & static conditions at each point was calculated. The results are shown in Fig. 12

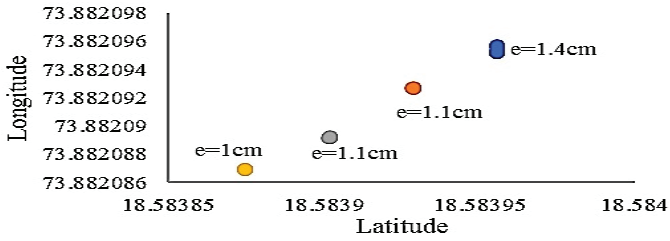

Figure 12. RTK accuracy in dynamic conditions.

3.8 Location Marking Accuracy Using Only INS in GNSS Denied Environment

In a GNSS-denied environment, the accuracy only depends on the INS estimates. The INS used in the experiment here has acceleration bias instability: <15µg, angular rate range: ±450°/s, angular bias instability: 0.8°/hr, roll accuracy: 0.06° RMS (static/low dynamics), pitch accuracy: 0.1° RMS (dynamic), heading accuracy: <0.3° RMS. Here, to simulate the condition, we have measured the INS data after disconnecting the GNSS Rover antenna from the Vehicle-mounted receiver. Initially, GNSS location details of Point 1 and 2 of Fig. 13 were marked on the ground surface at a distance of 3 m. GNSS antenna and receiver were mounted on the same platform so that the relative displacement between them was zero. The GNSS antenna was placed at Point 1. When RTK was achieved, the antenna was disconnected. Next, the INS data were recorded after they were stabilized to the extent that the changes in the value were not significant. Subsequently, the setup is moved from Point 1 to Point 2 in 5 sec and placed on Point 2. Instantly, the distance displayed on the GUI, is noted. The distance between Point 1 (pure GNSS) and Point 2 (only INS) is calculated. Now, the error between the calculated distance and the actual distance is determined. In addition, the maximum error after stabilization (it means that the rate of change of angular error reduces w.r.t. time to the extent where we have assumed it to be stable) of data and the time for stabilization were also recorded. Similarly, the tests for 6m and 12m were also carried out. Six sets of data were collected for each intermediate distance and the results are shown in Fig. 14. The results show that the errors in the GPS-denied environment are more than the baseline distances.

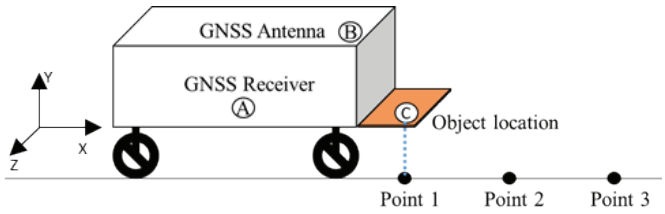

Figure 13. Setup for lever arm implementation.

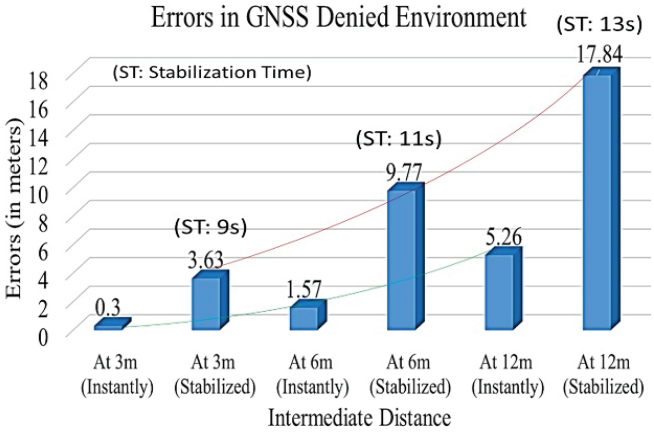

Figure 14. Errors in GNSS denied environment.

The Lever arm compensation was carried out using the GNSS case as per reference 15, where the position measurement of GNSS can be expressed as:

$$ZGNSS=PINS+\Xi C$$

$$Z_{GNSS} = P_{INS} + \Xi C_b^n r_b + v_{GNSS} \quad (4)$$

$$\Xi = \begin{pmatrix} \frac{1}{(R_m+h)} & 0 & 0 \\ 0 & \frac{1}{\{(R_t+h)*\cos L\}} & 0 \\ 0 & 0 & -1 \end{pmatrix} \quad (5)$$

The latitude L, longitude l, and height h are arranged as the vector P. The subscript INS indicates that it is the true position of the centre of the INS, as does GNSS. Ξ transforms the lever arm rb from the body frame to the geodetic coordinates L, l and h. The geodetic frame of GNSS with direction cosine matrix shows measurement noises of GPS. The rb is the offset from the INS to the GNSS antenna resolved in the body frame. Rm and Rt are meridian and normal radii of curvature of the earth's ellipsoid respectively. The [L lh]T is the position vector P in

Table 1. Lever arm correction coordinates

Offset from GNSS antenna to GNSS/INS	**X: -0.4m Y: -0.4m Z: +0m**	**Offset from GNSS/INS to Object location**	**X: +0.91m Y: +0.275m Z: +0.751m**
Point No.	**GNSS RTK location**	**Measured locations with lever arm**	**Error (in cm)**
	18.58438630N 73.88187066E	18.58438641N 73.88187067E	1.2
		18.58438634N 73.88187074E	2.5
		18.58438642N 73.88187060E	8.0
	18.58439025N 73.88184245E	18.58439001N 73.88184244E	0.95
		18.58439033N 73.88184257E	1.3
		18.58439022N 73.88184259E	7.3
	18.58439444N 73.88181452E	18.58439489N 73.88181392E	1.4
		18.58439450N 73.88181448E	1.5
		18.58439452N 73.88181450E	7.3

the local tangent plane. The estimated position of the same point will be given as:

$$Z_{INS} = P_{INS} + \Xi C_b^n r_b \quad (6)$$

The same was implemented for the Lever Arm compensation in the software, considering Rm and Rt as equal by taking earth as a spherical object and L has been taken as zero for ease of calculation. At this point, the location can be shifted from the GPS antenna to the Object location.

For testing purposes, three points were marked on the flat ground having a zero-degree slope (Fig. 14). Their locations were marked using the standalone GNSS. GNSS receiver (A) and GNSS antenna (B) were mounted at different locations on the trolley. The location of the object was to be marked as a third point (C) on the trolley, which is away from the GNSS receiver and GNSS antenna. The trolley was positioned such that the point (C) on the vehicle was exactly above the 1st point on the ground. The correctness of the object location after implementation of the lever arm corrections was verified by comparing the pure GNSS data recorded earlier with the output from INS. This experimentation was done for all three points marked on the ground. Results are shown in Table 1.

3.9 Error Correction on Slopes

To incorporate angle correction, Eqn. (4), (5), and (6) are used to calculate the position. Here, the latitude (L) will vary as per the slope angle. The Rover GNSS with INS was mounted

Table 2. Angle correction implementation

S. No.	**Angle (degrees)**			**GNSS-INS (GNSS Antenna 1)**	**GNSS (GNSS Antenna 2)**	**Error in cm**
	Roll	**Pitch**	**Course**			
Lifting the platform from Left side						
1	1.36	11.56	278.92	18.58444673 73.88159932	18.58444726 73.8815993	5.8
2	1.35	7.21	278.55	18.58444662 73.88159907	18.58444732 73.88159901	7.8
3	1.56	4.22	279.26	18.58444687 73.88159902	18.5844473 73.88159879	5.3
4	1.35	2.22	279.34	18.58444682 73.88159887	18.5844473 73.88159869	5.4
5	1.08	-1.29	279.2	18.58444675 73.88159869	18.58444739 73.88159842	7.6
Lifting the platform from Right side						
1	1.69	-1.21	277.24	18.58444673 73.88159854	18.58444721 73.88159837	5.5
2	1.38	-2.2	278.01	18.58444678 73.88159852	18.58444719 73.8815982	5.67
3	1.07	-4.22	277.88	18.5844468 73.88159847	18.58444725 73.88159803	6.8
4	0.99	-7.22	277.96	18.58444682 73.88159811	18.5844473 73.88159794	5.6
5	0.92	-14.34	277.75	18.58444702 73.88159751	18.58444742 73.88159732	4.8

on a platform. The receiver antenna (GNSS antenna-1) was mounted 1 metre above the platform. A second antenna (GNSS antenna-2) was mounted on the platform depicting the object's location. The lever arm component values of GNSS antenna 1 and object location (GNSS antenna 2) are measured and fed to the system. The platform was lifted from one end (either Right or Left) of the setup. Five points at different angles on each side were measured. The GNSS-INS reading of Antenna 1 provides slope-compensated values. The GNSS Antenna 2 (object location) provides a standalone GNSS reading, which is the correct value. The difference between the GNSS-INS value at the GNSS-INS antenna 1 point and the pure GNSS values at the GNSS antenna 2 point is the error in the system. Results are shown in Table 2. The angles are measured using INS sensors. Here, the calculated errors after slope compensation are within permissible limits of a few cm. These errors are mainly because of the manual positioning of the GNSS antennas and inherent errors of inertial sensors.

4. CONCLUSIONS

In defense ground applications, there is a requirement for high positional accuracy for static and dynamic platforms. To provide in-house solutions with such accuracies, evolving the test methodology and its performance evaluation become pertinent.

In our application, there are two types of errors: DGNSS inherent error in the RTK mode that affects in small amount, and error due to dynamics of platform contributing in large amount.

By understanding the various factors due to the platform dynamics degrading the accuracy, we evolved a test methodology to evaluate the DGNSS (RTK mode) performance for absolute and differential errors. The inherent error varies from 0.8 cm to 3.3 cm, compensating for ionospheric error, atmospheric error, multipath error, receiver noise, etc.

The dynamic errors include the position offsets and slope error correction. After implementing both the corrections, we could achieve accuracy better than 10 cm. It reduces uncertainties arising from the dynamics of the mechanical system. It will provide a much more accurate location of objects for casualty-free recovery.

However, in a GNSS-denied environment, it has been observed that the MEMS-based INS position error increases quadratically with time. For the short duration of GNSS outage during laying, MEMS-based INS may be used, but for applications like avionics and naval systems, where a longer duration of GNSS outage occurs, FOG / RLG-based INS should be used to decrease the divergence in positional accuracy.

REFERENCES

1. Gagandeep Purohit & Moiz Chasmai, Performance evaluation of DGNSS with RK corrections, IOSR-JECE, 2014, **9**(2), VI, 43-47
   doi: 10.9790/2834-09264347
2. Mallette, L. & Rochat, P. An introduction to satellite based atomic frequency standards. *In* Proceedings of IEEE Aerospace Conference 2008.
   doi: 10.1109/AERO.2008.4526366
3. Bonnor, N. A brief history of global navigation satellite systems. *J. Navig.,* 2012, **65**(1), 1
   doi: 10.1017/S0373463311000506
4. Catania, P. & Comparetti, A. Positioning accuracy comparison of GNSS receivers used for mapping and guidance of agricultural machines. *Agronomy*, 2020, **10**, 924
   doi: 10.3390/agronomy10070924
5. Jenos, D. & Kuras, P. Evaluation of low cost RTK GNSS receiver in motion under demanding conditions. *Measurem,* 2022, 0263-2241
   doi: 10.1016/j.measurement.2022.111647
6. Xue, C. & Psimoulis, P. Assessment of the accuracy of low-cost multi-GNSS receivers in monitoring dynamic response of structures, 2022. *Appl Geoma*.
   doi: 10.1007/s12518-022-00482-8
7. Xue, C. & Psimoulis, P.A. Feasibility analysis of the performance of low cost GNSS receivers in monitoring dynamic motion. *Measurem*, 2022, **11**, 1819
   doi: 10.1016/j.measurement.2022.111819
8. Rui Sun, L.J. & Cheng, Q. Evaluation of the performance of GNSS-based velocity estimation algorithms. *Satell. Navig.*, 2022, **3**(18).
   doi: 10.1186/s43020-022-00080-4
9. Teunissen, P.J.G. & Montenbruck, Springer handbook of GNSS, 2017
   doi: 10.1007/978-3-319-42928-1
10. Bansal, R. Deriving and testing the great circle theory. *Int. J. Statis Appl. Mathem.*, 2021 **6**(5), 16-24.
    doi: 10.22271/maths.2021.v6.i5a.722
11. Azdy, R.A. & Darnis, F. Use of haversine formula in finding distance between temp shelter and waste end sites. *In* Proceedings of Physics an Astronomy: General Physics and Astronomy. *J. Phys*. 2020, **1500**(012104).
    doi: 10.1088/1742-6596/1500/1/012104
12. Carroll, J. & Hughes, S. Using a video camera to measure the radius of the Earth. *Phys. Educ*., 2006, **48**(6), 731–735
    doi: 10.1088/0031-9120/48/6/731
13. Khodabandeh, K-Wang, A. A study on predicting network corrections in PPP-RTK processing. *Adv. Space Res.*, 2017, **60**(7), 1463-1477
    doi: 10.1016/j.asr.2017.06.043
14. Garcia, A.R. & Juan, J.M. Fast precise point positioning: A system to provide corrections for single and multi-frequency navigation. *Navigat*, 2016, **63**(3), 231-247
    doi: 10.1002/navi.148
15. Seo, J.; Lee, H.K.; Lee, J.G. & Park, C.G. Lever arm compensation for GPS/INS/Odometer integrated system, *J. Con, Auto & Sys*, 2006, **4**(2), 247-254
    doi: 10.5139/JKSAS.2013.41.6.481

CONTRIBUTORS

Mr Moiz Chasmai is a Scientist at DRDO-R&DE(E), Pune, India. His areas of interest include: D&D of electronic control systems and DGNSS/ INS - GIS-based navigation systems for combat applications.

For the current study, he was involved in the preparation of the abstract, system configuration, and finalisation of various parameters for performance evaluation. He has also prepared

the discussion and conclusion section. As a lead author, he has also carried out sequencing, drafting and editing of the script.

Mr Gagandeep Purohit is a Scientist at DRDO-R&DE(E), Pune, India. His areas of interest include: D&D of electromagnetic systems and DGNSS/ INS - GIS-based navigation systems for combat applications.
For the current study, he was involved in the preparation of navigation system hardware for location marking of the objects with required accuracy. He was also involved in analysing the data and preparation of the graphs.

Mr Arun Kumar Barde is a Scientist at DRDO-R&DE(E), Pune, India. His areas of interest include: D&D of electronic control systems for combat applications.
For the current study, he was involved in carrying out experiments for location marking accuracy using only INS in a GNSS-denied environment and error correction on slopes.

Mr Sandeep is a Senior Technical officer at DRDO-R&DE(E), Pune, India. His areas of interest include: Embedded systems design, PCB Prototyping and the development of ECAD software.
For the current study, he was involved in carrying out field testing and compilation of data for analysing the results.

Mr Prashant Kumar is a Senior Technical officer at DRDO-R&DE(E), Pune, India. His areas of interest include: Embedded systems design, electronic circuit design, PCB Prototyping and development of ECAD software.
For the current study, he was involved in carrying out field testing and compilation of data for analysing the results.

Mr Abhijit Kamble is a Senior Scientist at DRDO-R&DE(E), Pune, India. His areas of interest include: Control system design for ground-based military equipment.
For the current study, his contribution includes the layout of the script. He was also involved in analysing the data and preparing the graphs.